Available online at www.sciencedirect.com
ScienceDirect
Journal of Hazardous Materials 143 (2007) 516–521
Journal of Hazardous Materials
www.elsevier.com/locate/jhazmat

Effect of metal doping into $Ce_{0.5}Zr_{0.5}O_2$ on photocatalytic activity of $TiO_2/Ce_{0.45}Zr_{0.45}M_{0.1}O_X$ (M = Y, La, Mn)

Zhong Jun Bo, Lintao, Gong Maochu, Wang Jian Li, Liu Zhi Min, Zhao Ming, Yaoqiang Chen *

College of Chemistry, Sichuan University, Chengdu 610064, Sichuan, China

Received 27 June 2006; received in revised form 4 September 2006; accepted 22 September 2006
Available online 29 September 2006

Abstract

The paper demonstrates that the photocatalytic activity of TiO_2 towards the decomposition of gaseous benzene in a batch reactor can be greatly improved by loading TiO_2 on the surface of CeO_2–ZrO_2. The research investigates the effects of three metals doping into $Ce_{0.5}Zr_{0.5}O_2$ on photocatalytic activity of $TiO_2/Ce_{0.45}Zr_{0.45}M_{0.1}O_X$ (M = Y, La, Mn). The prepared photocatalysts were characterized by BET, XRD, UV–vis diffuse reflectance and XPS analyses. BET surface area of $TiO_2/Ce_{0.45}Zr_{0.45}M_{0.1}O_X$ (M = Y, La, Mn) is smaller than that of $Ce_{0.5}Zr_{0.5}O_2$. XRD results reveal that the deposited titania is highly dispersed as in the CeO_2–ZrO_2 matrix, doping *M* in the CeO_2–ZrO_2 lattice causes the changing of lattice space and the diffraction peaks shift to higher 2θ position. Among these four catalysts, the band gap value of $TiO_2/Ce_{0.45}Zr_{0.45}La_{0.1}O_X$ is the lowest. The binding energy value of Ti $2p_{3/2}$ of four catalysts transfers to a lower value. The order of photocatalytic activity is $TiO_2/Ce_{0.45}Zr_{0.45}La_{0.1}O_X > TiO_2/Ce_{0.45}Zr_{0.45}Y_{0.1}O_X > TiO_2/Ce_{0.45}Zr_{0.45}Mn_{0.1}O_X > TiO_2/Ce_{0.5}Zr_{0.5}O_2 > TiO_2$. The proposed mechanism is of electron transfer and the stronger absorption in the region 210–400 nm.
© 2006 Elsevier B.V. All rights reserved.

Keywords: TiO_2; Benzene; Ceria–zirconia mixed oxides; Photocatalytic oxidation; Gas-phase; Doping

1. Introduction

In recent years, environment legislation has imposed stringent limits on atmospheric emission levels. In particular, the release of volatile organic compounds (VOCs) has received much attention [1]. The volatile organic compounds are widely used in industrial process and domestic activities. These extensive uses lead to water and air pollution, particularly in indoor air pollution. Many VOCs are known to be toxic and considered to be carcinogenic. The most significant problem related to the emission of VOCs is centered on the potential production of photochemical oxidants; for example, ozone and peroxyacetyl nitrate [2]. Emissions of VOCs also contribute to localized pollution problems of toxicity and odor. Many VOCs are implicated in the depletion of the stratospheric ozone layer and may contribute to global warming [3].

As a result of all these problems, VOCs have drawn considerable attention in recent years. Conventional methods for treating VOCs from gas streams, such as absorption, adsorption, condensation, thermal/catalytic incineration, biological processes and stream reforming all have inherent limitations and none are definitely cost-effective [2,4]. Among the technologies developed for the treatment of VOCs, the photocatalytic oxidation process is considered to be a promising technology. The attractive advantages of this technology are: (i) photocatalytic oxidation can proceed at ambient temperature and pressure; (ii) the excitation source can be sunlight or low-cost fluorescent light source; (iii) photocatalysts are generally nontoxic, inexpensive, and chemically and physically stable; (iv) final oxidation products are usually innocuous; (v) no additives required (only oxygen from the air) [5,6]. It is likely that this technology in air purification reveals strong advantages and capacious application foreground, but deactivation of the titanium dioxide catalyst during gas–solid photocatalytic oxidation of air contaminated by VOCs is a serious issue and deserves attention from industrial application and academic researchers [7].

Sauer et al. [8] investigated the gas-phase photocatalytic reaction of benzene in a recirculation photocatalytic sys-

* Corresponding author. Tel.: +86 28 85418451; fax: +86 28 85418451.
E-mail addresses: zhongjunbo@Sohu.Com, scuzhong@sina.com (Z.J. Bo), liuzhimin2648@Sina.Com (L.Z. Min).

0304-3894/$ – see front matter © 2006 Elsevier B.V. All rights reserved.
doi:10.1016/j.jhazmat.2006.09.071

tem. Their results showed that the concentration of benzene clearly decreased when the initial concentration was less than 100 mg/m^3, with no change detected after 140 min when the initial concentration up to 300 mg/m^3, there is hence no photocatalytic activity for higher concentration of benzene. Hennezel et al. [9] noted catalyst deactivation for a toluene and perchloroethylene feed mixture in air. Kim et al. [10] treated TiO_2 with water and HCl, and noticed that when the concentration of benzene was 50 mg/m^3, benzene conversion over TiO_2/H_2O reached 80% and dropped slowly to 30% in about 3 h because of deactivation of photocatalyst. The benzene conversion over TiO_2/HCl remained nearly constant at about 25% for the entire 6 h run due to its low photocatalytic activity.

The decomposition of volatile organic compounds has been difficult because of the low conversion and the common deactivation of photocatalyst. Therefore, it is crucial to prolong the lifetime of the photocatalyst and enhance its photocatalytic activity. Various techniques have been developed for development and modification of the TiO_2-based photocatalysts [11].

Nowadays, CeO_2–ZrO_2 is one of the most important commercial catalytic supports due to its use in the three way catalysts [12]. It is applied in these systems owing to its high oxygen storage capacity. This material has been investigated since the early 1990s and is now generally known that the incorporation of zirconium into the ceria lattice creates a higher concentration of defects improving, thus, the O^{2-} mobility; such mobility would explain the outstanding ability to store and release oxygen [13]. However, to our knowledge, there are few reports on the effect of metal doping into $Ce_{0.5}Zr_{0.5}O_2$ on photocatalytic activity of $TiO_2/Ce_{0.45}Zr_{0.45}M_{0.1}O_X$.

Benzene is a major indoor and industrial air pollutant, and it was recommended as one of eight representative indoor VOCs. In the present paper, benzene was therefore chosen as the model VOC to investigate the capability with $TiO_2/Ce_{0.45}Zr_{0.45}M_{0.1}O_X$. The objective of this work is to investigate the effect of three metals doping into $Ce_{0.5}Zr_{0.5}O_2$ on photocatalytic activity of $TiO_2/Ce_{0.45}Zr_{0.45}M_{0.1}O_X$ (M = Y, La, Mn). This paper presents the experimental results and discusses the influence of three metals doping into $Ce_{0.5}Zr_{0.5}O_2$ on photocatalytic activity.

2. Experimental

2.1. Preparation of $TiO_2/Ce_{0.45}Zr_{0.45}M_{0.1}O_X$ (M = Y, La, Mn)

All reagents, AR grade, were purchased from Chendu Kelong Chemical Reagents Factory and used as received. Deionized water was used throughout the experiments.

$Ce_{0.5}Zr_{0.5}O_2$ and $Ce_{0.45}Zr_{0.45}M_{0.1}O_X$ were prepared by coprecipitation with $NH_3{\cdot}H_2O$ and $(NH_4)_2CO_3$ mixed $Ce(NO_3)_3$, $ZrOCO_3$, $Mn(NO_3)_2$, $Y(NO_3)_3$, $La(NO_3)_3$ aqueous solutions with a nominal composition. The precipitate was filtered, washed with distilled water until no pH change could be detected, then calcined in air at 873 K for 4 h in a muffle furnace. These samples $Ce_{0.5}Zr_{0.5}O_2$, $Ce_{0.45}Zr_{0.45}Y_{0.1}O_X$, $Ce_{0.45}Zr_{0.45}La_{0.1}O_X$ and $Ce_{0.45}Zr_{0.45}Mn_{0.1}O_X$ (all called CeO_2–ZrO_2) are labeled as 1#, 2#, 3#, 4#, respectively.

Precursor solution for TiO_2 was prepared by the following method. Tetrabutylorthotitanate (17.2 mL) and diethanolamine (4.8 mL) were dissolved in ethanol (67.28 mL). After stirring vigorously for 2 h at room temperature, a mixed solution of water (0.9 mL) and ethanol (10 mL) was added dropwise to the above solution under stirring. The resultant alkoxide solution was kept standing at room temperature for hydrolysis during 2 h, resulting in the TiO_2 sol. The composition ratio of Ti $(OC_4H_9)_4$, C_2H_5OH, H_2O and NH $(C_2H_4OH)_2$ in the starting alkoxide solution was 1:26.5:1:1 (in molar ratio). The pure TiO_2 powder was prepared after calcination the TiO_2 gel at 773 K.

The photocatalyst of TiO_2/CeO_2–ZrO_2 with 1 wt% of TiO_2 loading were prepared by impregnating method using TiO_2 sol, then cacinated at 773 K for 2 h. TiO_2 loaded on $Ce_{0.5}Zr_{0.5}O_2$, $Ce_{0.45}Zr_{0.45}Y_{0.1}O_X$, $Ce_{0.45}Zr_{0.45}La_{0.1}O_X$ and $Ce_{0.45}Zr_{0.45}Mn_{0.1}O_X$ is designated as C1, C2, C3, C4, respectively.

2.2. Characterization of $TiO_2/Ce_{0.45}Zr_{0.45}M_{0.1}O_X$

Surface area analysis of TiO_2/CeO_2–ZrO_2 was carried out by the Brunauer-Emmet Teller (BET) method using Autosorb-ZXF-05 (Xibei Chemical Institute, China). The samples were evacuated 3 h at 623 K, then cooled to 77 K using liquid N_2 at which point N_2 adsorption was measured. X-ray diffraction patterns were recorded with a DX-1000 X-ray diffraction (XRD) using Cu/Kα radiation, 40 kV, 20 mA. XPS measurement was carried out on a spectrometer (XSAM-800, KRATOS Co.) with Mg Kα anticathode. The UV–vis diffuse reflectance spectrum was performed on a spectrometer (TU-1907). Total oxygen storage capacity (OSC) was measured after reducing the catalyst (200 mg) at the appropriate temperature (823 K) under H_2 flow (40 mins). Before measuring O_2 uptake, the catalyst after reduction was cooled to 473 K under N_2 flow, and then pulse of oxygen were injected up to the breakthrough point. OSC was evaluated from oxygen consumption.

2.3. Evaluation of the photocatalysis

Experiments were carried out in a closed stainless steel reactor with the volume of 105 L (50 cm (H) × 46 cm (L) × 46 cm (W)). An electric fan and three 10 W black light lamps with maximum wavelength of 365 nm were installed on a bracket (see Fig. 1). Twenty grams of photocatalyst powder was dispersed in a thin layer over two aluminum foils with the total area of 980 cm^2 (2 × 24.5 cm (L) × 20 cm (W)), and the required quantity of liquid benzene was injected into the reactor. The vertical distance between light and aluminum foil is 15 cm, 30 cm, 45 cm, respectively. Once dark-adsorption equilibrium has been reached, photocatalysis is started by turning on the UV light source. The initial concentration of benzene was kept at 400 mg/m^3 for all the experiments. The photocatalytic oxidation of benzene was performed under illumination at 312–313 K to avoid condensation of benzene by placing two infrared lamps outside the reactor. The concentration of benzene was detected

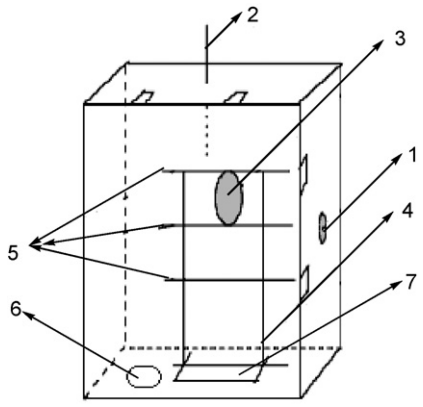

Fig. 1. Schematic diagram of the batch photocatalytic reactor: (1) sampling point, (2) thermometer, (3) electric fan, (4) bracket, (5) black light lamp, (6) hygrometer and (7) aluminum foil.

by gas-phase chromatogram with FID detector and GDX-101 chromapack column. The gas was withdrawn regularly from the reactor for analysis.

In this paper, the conversion rate was calculated by $(C_0 - C)/C_0$, where C is the concentration of the reactant after irradiation as a function of reaction time and C_0 is the concentration of the reactant after adsorption equilibrium and before the irradiation in the presence of catalyst.

3. Results and discussion

3.1. BET surface area, pore size, pore volume and OSC

The surface parameter and OSC of the catalysts are shown in Table 1. Compared with C1, BET surface area, pore volume and pore size of C2–C4 decrease. Among these four photocatalysts, C3 has the lowest BET surface area, pore volume and pore size. As for OSC, C3 has the lowest OSC, C4 has the highest OSC, it is plausible that MnO_X also is a kind of oxygen storage material, MnO_X can store/release oxygen [15].

3.2. XRD characterization

The X-ray diffraction patterns of the as-received photocatalysts powder sample are shown in Fig. 2. Only the cubic phase of CeO_2–ZrO_2 was observed in photocatalyst samples. The peaks of titania in either rutile or anatase form are not detected by XRD in the 2θ region from 20° to 50°, which indicates that the deposited titania is highly dispersed as in the support matrix. As

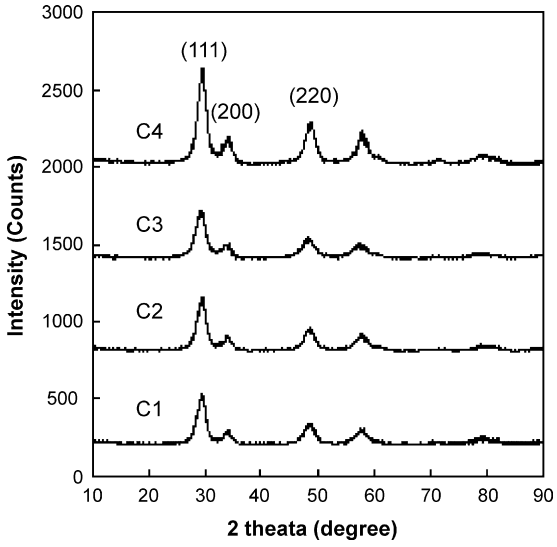

Fig. 2. XRD patterns of TiO_2/CeO_2–ZrO_2.

shown in Fig. 2, doping M in the $Ce_{0.5}Zr_{0.5}O_2$ lattice causes the change of lattice space and the diffraction peaks to shift to higher 2θ position. The particle size of these samples, D_{XRD} was calculated according to the Scherrer equation: $D = 0.92\lambda/B\cos\theta$, where λ is the wavelength of the radiation, θ the diffraction angle, and B is the corrected half-width of the diffraction peak. The results of the particle size are presented in Table 2.

3.3. UV–vis diffuse reflectance characterization

Since the pure and loaded titanina samples were prepared for use in the photocatalytic reaction, their UV–vis diffuse reflective properties may have had a strong effect on the photocatalytic activity. Fig. 3 shows the diffuse reflectance spectrum of pure and loaded TiO_2.

As shown in Fig. 3, from 210 nm to 400 nm, C1, C2, C3, C4 have no obvious difference. Compared with TiO_2, C1–C4 shows red shift. It is obvious that the presence of CeO_2–ZrO_2 clearly changes the spectra of TiO_2 in the ultraviolet light region.

The band gap of the samples was determined by the equation $E_g = 1239.8/\lambda$, where E_g is the band gap (eV) and λ (nm) is the wavelength of the absorption edges in the spectrum [16]. The results are presented in Table 3.

As shown in Table 3, among these four catalysts, band gap of C3 is the lowest, which indicates that T3 has the best photocatalytic activity under same irradiation condition. This result is in agreement with the results of photoactivity.

Table 1
Surface parameter and OSC of the catalysts

Catalysts	S_{BET} (m^2/g)	Pore volumes (cm^3/g)	Pore sizes (nm)	OSC (μmol/g)
C1	86.59	0.18	3.77	532.70
C2	85.90	0.16	3.54	418.92
C3	64.60	0.12	3.12	323.37
C4	71.54	0.14	3.31	770.55

Table 2
Particle size of the photocatalysts

Catalysts	Particle sizes (nm)		
	(1 1 1)	(2 0 0)	(2 2 0)
C1	4.7	4.7	4.0
C2	4.4	4.3	3.9
C3	4.0	3.8	3.4
C4	4.4	5.4	4.3

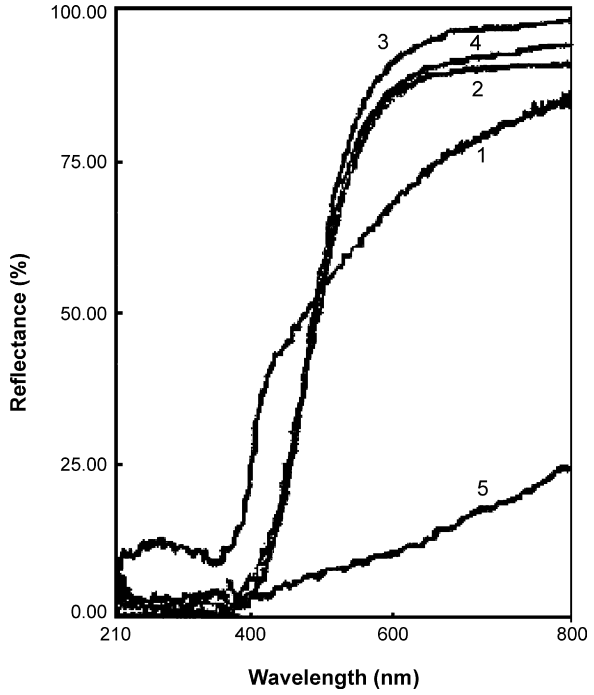

Fig. 3. UV–vis diffuse reflectance spectra (1) TiO_2, (2) C1, (3) C2, (4) C3, and (5) C4.

3.4. XPS characterization

The XPS spectrum shows that there are Ti, O, C elements on all the surface of the TiO_2/CeO_2–ZrO_2 samples besides Ce, Zr, M elements. Element Ti is resulted from the precursor solution. Element O is assigned to the precursor solution and CeO_2–ZrO_2. The C element probably came from the organic radicals of precursor for sol–gel method, which were not completely burnt out during heat-treatment. The data of Ti 2p are presented in Table 4.

As shown in Table 4, for pure TiO_2 and C4, the binding energy difference, $\Delta E_b = E_b(\text{Ti } 2p_{1/2}) - E_b(\text{Ti } 2p_{3/2})$ is 5.7 eV, as previously reported in the literature [14]. However, for C1, C2, C3, only Ti $2p_{1/2}$ was observed, but the binding energy value of Ti $2p_{3/2}$ of four catalysts transfer to a lower value, the result indicates that Ti forms strong radical links through oxygen bridges with CeO_2–ZrO_2. So it is obvious that there is stronger interaction between CeO_2–ZrO_2 and TiO_2. Among the four catalysts, binding energy value of Ti $2p_{3/2}$ of C3 transfers to the lowest value, which implies that the interaction between $Ce_{0.5}Zr_{0.5}O_2$ and TiO_2 of C3 is the strongest and the promotion effect on catalytic activity of TiO_2 is perhaps the biggest as well.

Table 3
Absorption edges and band gaps of the photocatalysts

Catalysts	First absorption edge (nm)	Band gap (eV)	Second absorption edge (nm)	Band gap (eV)
C1	422	2.94	500	2.48
C2	420	2.95	490	2.53
C3	430	2.88	475	2.61
C4	–		–	

Table 4
Peak fitting results of the high resolution spectra of the Ti 2p

Catalysts	Binding energies of Ti 2p (eV)		
	E_b (Ti $2p_{1/2}$)	E_b (Ti $2p_{3/2}$)	ΔE_b
TiO_2	464.6	458.9	5.7
C1	–	458.3	–
C2	–	458.3	–
C3	–	458.2	–
C4	464.0	458.3	5.7

3.5. Blank experiments

The reference experiments were carried out in three conditions: the first with illumination but no catalyst, the second with TiO_2 (pure TiO_2 and loaded TiO_2) but no illumination, the third with illumination over four supports. The results show that the concentration of benzene (400 mg/m^3) change so little under these conditions that conversion can be ignored. The blank tests proved the stability of benzene rings. Without illumination or photocatalyst, benzene is thermodynamically stable. It is also suggested that dark adsorption for benzene from gas phase is small; therefore the adsorption equilibrium can be established quickly.

3.6. photocatalytic activity of TiO_2/CeO_2–ZrO_2

The photocatalytic activity of TiO_2/CeO_2–ZrO_2 and 0.2 g pure TiO_2 (S_{BET} is 76.68 m^2/g) are compared and presented in Fig. 4.

As shown in Fig. 4, the order of photocatalytic activity is C3 > C2 > C4 > C1 > TiO_2. In the process of decomposing, the pure TiO_2 deactivates after 1.5 h and the maximum conversion of 16.2% is reached at moment of 1.5 h, while the loaded catalyst exhibits its superiority stability. For C3, in the whole process of reaction, the conversion rate keeps increasing until 2.5 h when the photocatalytic activity begins to decline and the maximum conversion of 46.72% is reached. Moreover, the conversion rate is about 2.88 times that of the pure TiO_2. For C2, C4, C1, the conversion rate is 39.63%, 30.0%, 24.9%, respectively, and the

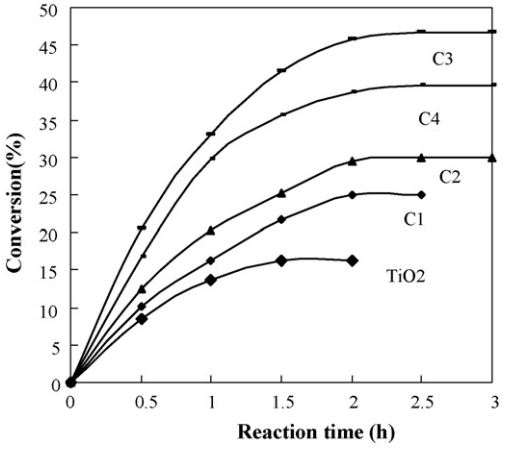

Fig. 4. Conversion of benzene vs. time (Relative Humidity (RH): 50%).

deactive time is 2.5 h, 2.0 h, 2.0 h, respectively. It is clear that the TiO_2 loaded on CeO_2–ZrO_2 can prolong the life of photocatalyst and enhance the photocatalytic activity of catalyst. Moreover, photocatalytic activity of $TiO_2/Ce_{0.45}Zr_{0.45}M_{0.1}O_X$ (M = Y, La, Mn) is better than that of $TiO_2/Ce_{0.5}Zr_{0.5}O_2$. It is plausible that this result can be contributed to the following fact. Doping metal into $Ce_{0.5}Zr_{0.5}O_2$ can increase more crystal defects than $Ce_{0.5}Zr_{0.5}O_2$ and oxygen cavities on surface of $Ce_{0.45}Zr_{0.45}M_{0.1}O_X$ (M = Y, La, Mn) is more than those on surface of $Ce_{0.5}Zr_{0.5}O_2$. Since oxygen cavity can capture electron which is excited from the valence to the conduction, so the recombination of electron-hole pairs can be impeded, thus more holes can be used.

As seen from the above results, it is seen that there is no direct correlation between photocatalytic activity and OSC. The photocatalytic process mainly occurs on the surface of the photocatalyst and adsorption precedes photodegradation. The OSC not mainly depends on the surface but the bulk [12]. Hence factors like colloidal size and surface that influence the adsorption in turn can also influence the photacatalytic activity.

The photocatalytic activity of TiO_2 is not high enough to be useful for industrial purpose [17]. Several methods have been attempted to improve the photocatalytic efficiency, such as impeding the recombination of electron-hole pairs and enhancing of visible light response [18]. In this paper, TiO_2/CeO_2–ZrO_2 exhibits stronger photocatalytic activity than pure TiO_2. It is plausible that stronger photocatalytic activity of TiO_2/CeO_2–ZrO_2 results from two factors.

The first factor is that the presence of CeO_2–ZrO_2 can prolong the life of electron-hole pairs and impede the recombination of electron-hole pairs. To explain the higher oxygen mobility of oxygen in ceria–zirconia oxides, researchers developed Oxygen Species mechanism [19–25]. The Oxygen Species mechanism presented in following:

$$O_{2gas} \rightarrow O_{2ads} \rightarrow O_{2ads}{}^{-}\ (\text{superoxide})$$
$$\rightarrow O_{2ads}{}^{2-}\ (\text{peroxide}) \rightarrow 2\,O_{2ads}{}^{-} \rightarrow 2O_{lattice}{}^{2-}$$

Considering the mechanism of photocatalytic reaction, when TiO_2 absorbs photons (recall the light with maximum wavelength of 365 nm), electrons is excited from the valence to the conduction band leaving holes behind. On one hand, excited electrons react with oxygen adsorbed on the surface of TiO_2, $O_{2ads}{}^{-}$ forms on the surface of TiO_2. In the present paper, CeO_2–ZrO_2 was used as support, TiO_2 was loaded on the surface of CeO_2–ZrO_2, if $O_{2ads}{}^{-}$ formed on the surface of TiO_2 transfers to the surface of CeO_2–ZrO_2, thus the recombination of electron-hole pairs can be impeded; on the other hand, if excited electrons transfer from the surface of TiO_2 to the surface of CeO_2–ZrO_2, the recombination of electron-hole pairs can also be impeded. Electrons transfer results in promotion the photocatalytic activity of TiO_2. The electron transfer mechanism is shown in Fig. 5.

The second factor is TiO_2/CeO_2–ZrO_2 increases the absorption from 210 to 400 nm, thus the photocatalytic activity can be promoted.

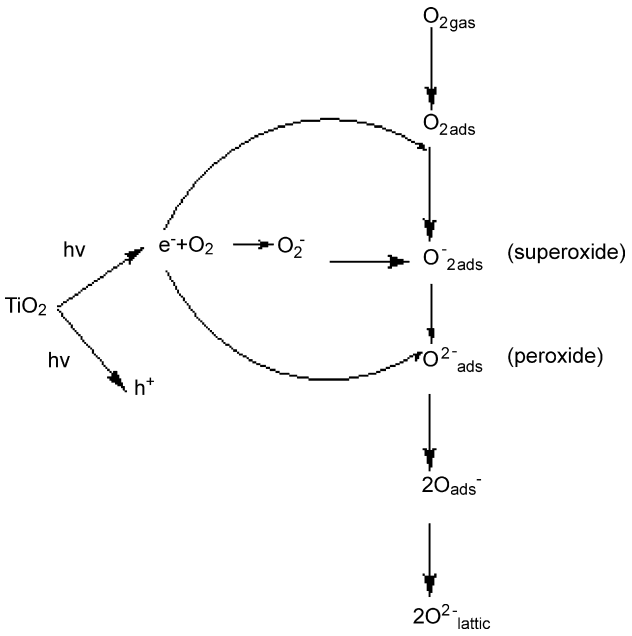

Fig. 5. Scheme depicting electron transfer of TiO_2/CeO_2–ZrO_2.

In fact, related factors all influence the photacatalytic activity. As a synergistic action results, C3 exhibits the best photacatalytic activity, C1 exhibits the worst photocatalytic activity.

4. Conclusions

In this paper, effect of three metal doping on photocatalytic activity of $TiO_2/Ce_{0.45}Zr_{0.45}M_{0.1}O_X$ (M = Y, La, Mn) was investigated. BET surface area of $TiO_2/Ce_{0.45}Zr_{0.45}M_{0.1}O_X$ (M = Y, La, Mn) is smaller than that of $Ce_{0.5}Zr_{0.5}O_2$. XRD results reveal that the deposited titania is highly dispersed as in the CeO_2–ZrO_2 matrix, doping M in the CeO_2–ZrO_2 lattice causes the lattice spacing to change and the diffraction peaks to shift to higher 2θ position. Among these four catalysts, band gap of $TiO_2/Ce_{0.45}Zr_{0.45}La_{0.1}O_X$ is the lowest. The binding energy value of Ti $2p_{3/2}$ of four catalysts transfers to a lower value. The order of photocatalytic activity is C3 > C2 > C4 > C1 > TiO_2. The proposed mechanism is of electron transfer and the stronger absorption in the region 210–400 nm.

References

[1] F. Bertinchamps, M. Trinen, N. Blangenois, E. Mariage, E.M. Gaigneaux, Positive effect of NOx on the performance of VO*x*/TiO2-based catalysis in the total oxidation abatement of chlorobenzene, J. Catal. 230 (2005) 493–498.
[2] S.B. Kim, S.C. Hong, Kinetic study for photocatalytic degradation of volatile organic compounds in air using thin film TiO_2 photocatalyst, Appl. Catal. B: Environ. 35 (2002) 305–315.
[3] R.M. Alberic, W.F. Jardim, Photocatalytic destruction of VOCs in the gas-phase using titanium dioxide, Appl. Catal. B: Environ. 14 (1997) 55–68.
[4] J.H. Wang, M.B. Ray, M. Bhowmick, Application of ultraviolet photooxidation to remove organic pollutants in the gas phase, Sep. Purif. Technol. 19 (2000) 11–20.
[5] H. Einaga, S. Futamura, T. Ibusuki, Heterogeneous photocatalytic oxidation of benzene, toluene, cyclohexene and cyclohexane in humidified air:

comparison of decomposition behavior on photoirradiated TiO_2 catalyst, Appl. Catal. B: Environ. 38 (2002) 215–225.
[6] M.M. Ameen, G.B. Raupp, B. Gregory, Reversible catalyst deactivation in the photocatalytic oxidation of dilute*o*-xylene in air, J. Catal. 184 (1999) 112–122.
[7] Q.C. Zhang, F.Y. Zhang, G.L. Zhang, X.P. Zhang, Gas-phase photo catalytic reaction properties of benzene on TiO_2, Chin. Environ. Sci. 23 (2003) 661–664.
[8] M.L. Sauer, M.A. Hale, D.F. Ollis, Heterogeneous photocatalytic oxidation of dilute toluene-chlorocarbon mixtures in air, J. Photochem. Photobiol. A: Chem. 88 (1995) 169–178.
[9] O.D. Hennezel, P. Pichat, D.F. Ollis, Benzene and toluene gas-phase photocatalytic degradation over H_2O and HCL pretreated TiO_2:by-products and mechanisms, J. Photochem. Photobiol. A: Chem. 118 (1998) 197–204.
[10] T.K. Kim, M.N. Lee, S.H. Lee, Y.C. Park, C.K. Jung, J.H. Boo, Development of surface cating technology of TiO_2 powder and improvement of photocatalytic activity by surface modification, Thin Solid Films 475 (2005) 171–177.
[11] A. Trovarelli, M. Boaro, E. Rocchini, C.D. Leitenburg, G. Dolcetti, Some recent developments in the characterization of ceria-based catalysts, J. Alloys Comp. 584 (2001) 323–324.
[12] P. Fornasiero, R.D. Monte, G. Rao, J. Kaspar, S. Meriani, A. Trovarelli, J. Graziani, Rh-loaded CeO_2-ZrO_2 solid-solutions as highly efficient oxygen exchangers: dependence of the reduction behavior and the oxygen storage capacity on the structural-properties, J. Catal. 151 (1995) 168–177.
[13] Y. Nagai, T. Yamamoto, T. Tanaka, S. Yoshida, T. Nonaka, T. Okamoto, A. Suda, M. Sugiura, X-ray absorption fine structure analysis of local structure of CeO_2-ZrO_2 mixed oxides with the same composition ratio (Ce/Zr = 1), Catal. Today 74 (2002) 225–234.
[14] J.G. Yu, X.J. Zhao, Q.N. Zhao, J.C. Du, Chin XPS of study of TiO_2 photocatalytic thin film prepared by the sol-gel method, Chin. J. Mater. Res. 14 (2000) 203–209.
[15] A.E. Nelson, K.H. Schulz, Surface chemistry and microstructural analysis of $Ce_xZr_{1-x}O_{2-y}$ model catalyst surfaces, Appl. Surf. Sci. 210 (2003) 206–221.
[16] A.R. Gandhe, J.B. Fernandes, A simple method to synthesize N-doped rutile tiania with enhanced photpcatalytic activity in sunlight, J. Solid State Chem. 178 (2005) 2953–2957.
[17] T.K. Young, Y.S. Kang, I.L. Wan, J.C. Guang, R.D. Young, Photocatalytic behavior of WO_3-loaded TiO_2 in an oxidation reaction, J. Catal. 191 (2000) 192–199.
[18] P. Bonamali, M. Sharon, G. Nogami, Preparation and characterization of TiO_2/Fe_2O_3 binary mixed oxides and its photocatalytic properties, Mater. Chem. Phys. 59 (1999) 254–261.
[19] C. Li, K. Domen, K.I. Maruya, T. Onishi, Dioxygen adsorption on well-outgassed and partially reduced cerium oxide studied by FT-IR, J. Am. Chem. Soc. 111 (1989) 7683–7687.
[20] C. Li, K. Domen, K.I. Maruya, T. Onishi, Oxygen exchange reaction over cerium oxide: an FT-IR study, J. Catal. 123 (1990) 436–442.
[21] D. Martin, D. Duprez, Mobility of surface species on oxide.1. Isotopic exchange of $^{18}O_2$ with ^{16}O of SiO_2, Al_2O_3, ZrO_2, MgO, CeO_2 and CeO_2-Al_2O_3, activation by noble metals, correlation with oxide basicity, J. Phys. Chem. 100 (1996) 9429–9438.
[22] Y. Madier, C. Descorme, A.M. Govie, D. Duprez, Oxygen mobility in CeO_2 and $Ce_xZr_{1-X}O_2$ compounds: study by CO transient oxidation and $^{18}O/^{16}O$ isotopic exchange, J. Phys. Chem. B 103 (1999) 10999–11006.
[23] C. Binet, M. Daturi, Lavalley, J. Claude, IR study of polycrystalline ceria properties in oxidised and reduced states, Catal. Today 50 (1999) 207–225.
[24] C. Descorme, Y. Madier, D. Duprez, Infrared study of oxygen adsorption and activation on cerium–zirconium mixed oxide, J. Catal. 196 (2000) 167–173.
[25] P.S. Lambrou, A.M. Efstathiou, The effects of Fe on the oxygen storage and release properties of model Pd–Rh/CeO_2–Al_2O_3 three-way catalyst, J. Catal. 240 (2006) 182–193.